Production of liquid hydrocarbons, carbon nanotubes and hydrogen rich gases from waste plastic in a multi-core reactor

Article *in* Journal of Analytical and Applied Pyrolysis · April 2017

DOI: 10.1016/j.jaap.2017.04.016

CITATIONS
27

READS
752

5 authors, including:

Ganesh Bajad
UICT, North Maharashtra University, Jalgaon, India
10 PUBLICATIONS **179** CITATIONS
SEE PROFILE

Vijayakumar R P
Visvesvaraya National Institute of Technology
30 PUBLICATIONS **525** CITATIONS
SEE PROFILE

Ajay Gama Gupta
Visvesvaraya National Institute of Technology
2 PUBLICATIONS **27** CITATIONS
SEE PROFILE

Journal of Analytical and Applied Pyrolysis 125 (2017) 83–90

Contents lists available at ScienceDirect

Journal of Analytical and Applied Pyrolysis

journal homepage: www.elsevier.com/locate/jaap

Production of liquid hydrocarbons, carbon nanotubes and hydrogen rich gases from waste plastic in a multi-core reactor

Ganesh S. Bajad, R.P. Vijayakumar*, Ajay G. Gupta, Vishakha Jagtap, Yogendra pal Singh

Department of Chemical Engineering, Visvesvaraya National Institute of Technology, Nagpur 440010, India

ARTICLE INFO

Keywords:
Multi–core reactor
Pyrolysis
Polyethylene
Carbon nanotubes
Hydrogen–rich gases

ABSTRACT

In this paper, a new reactor design based on central core heating system is presented that optimized the heat utilization and allowed compact reactor design. Conversion of waste plastic into liquid hydrocarbons, carbon nanotubes (CNTs) and hydrogen rich gases in a multi–core reactor was carried out. Thermal energy from central core was utilized for the pyrolysis of waste plastic and synthesis of CNTs. Pyrolysis of waste plastic was carried out in the outer chamber of reactor followed by catalytic decomposition of pyrolysis gases in the inner chamber. Tray arrangement inside CNT chamber provided maximum catalyst holdup and effective solid–gas contact. Reactor performance was studied at different pyrolysis temperatures and a fixed CNT synthesis temperature of 800 °C. Multi walled carbon nanotubes (MWCNTs) having 20–50 nm diameters and average wall thickness of 10 nm were synthesized with an yield of 6.03 g/30 g polyethylene.

1. Introduction

Pyrolysis of plastic gives a huge source of hydrocarbon and can be converted to carbon nanotubes (CNTs) using a suitable catalyst [1]. An economic production of CNTs using waste plastic as a precursor can develop nanotechnology based industries such as solar cells [2], batteries [3] polymer composites [3–5], electronic devices and displays [6,7].

In the commercial application of CNTs, challenges remains with purity, morphology and capital costs for the large–scale production of CNT from plastic waste [8]. Methods for large–scale synthesis of CNTs includes arc discharge [9], laser ablation method [10], chemical vapour deposition (CVD) [11–16], flame synthesis and combustion method. CVD was found to be the most economical and preferred method for large–scale synthesis of CNTs [11,17].

Zhou et al. [18,19] reported that, HDPE and LDPE as a carbon source gives same quality of CNTs synthesized using quartz tube reactor. Liu et al. [20] reported continuous production of CNTs using two–stage reactor, where the plastic waste pyrolysis and CNT synthesis was carried out in two separate units. Synthesis of CNTs using bubbling fluidized bed reactor gives uniform isothermal conditions due to effective solid gas contact, which increases the conversion rate of CNTs [21–24]. However, continuous fluidization using nitrogen and hydrogen gas leads more operating cost. CVD method using fixed bed reactor still has unsolved problems like maximum exposure of catalyst surface and utilization of entire hydrocarbons from the gaseous stream [8]. It is customary to utilize entire hydrocarbons generated from waste plastic pyrolysis to make the process eco–friendly.

Synthesis of CNTs using plastic waste needs the development of innovative materials and methods to reduce materials, capital cost and energy consumption. In view of these, the present work deals with conversion of waste plastic to liquid hydrocarbons, carbon nanotubes and hydrogen–rich–hydrocarbon gases using multi–core reactor. In this design, two reactors were coupled into singe reactor system having multiple cores. Heating media was provided in the annulus of inner and outer zone to heat both the chambers and lessen energy need. Multiple trays in the CNT chamber provided maximum catalyst loading and effective contact between solid and gases.

2. Material and methods

2.1. Materials

The oil recovery and CNT synthesis were carried out using post consumer edible oilcans made up of high–density polyethylene. Ni/Mo/MgO catalyst of mole ratio 4/0.2/1 was prepared by dissolving desired amount of $Ni(NO_3)_2{\cdot}6H_2O$, $(NH_4)_6Mo_7O_{24}{\cdot}4H_2O$, $Mg(NO_3)_2{\cdot}6H_2O$ and 2 g citric acid in 50 ml of deionized water. Chemicals were purchased from Merck specialties Pvt. Ltd with 99% purity.

* Corresponding author.
E-mail address: vijayakumarrp@che.vnit.ac.in (R.P. Vijayakumar).

http://dx.doi.org/10.1016/j.jaap.2017.04.016
Received 2 September 2016; Received in revised form 16 December 2016; Accepted 9 April 2017
Available online 24 April 2017
0165-2370/

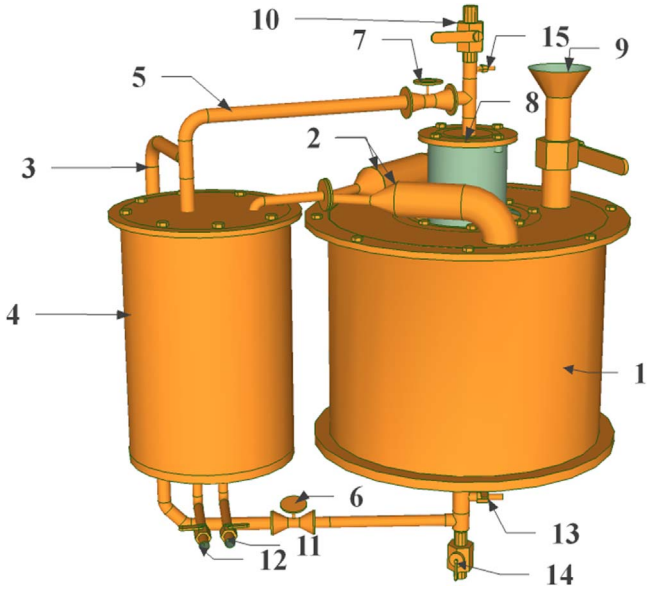

Fig. 1. Front view of multi–core reactor to produce fuel oil and CNTs using waste plastic as precursor. (1 – pyrolysis chamber, 2 – pyrolysis gases to condenser, 3 – gas outlet from condenser to CNT chamber, 4 – condenser, 5 – optional gas line, 6 & 7 – needle valve, 14 – off gas valve (for down draft flow), 8 – CNT chamber, 9 – feed hopper for plastic, 10 – off gas valve (for up draft flow), 11 – water drain, 12 – oil drain, 13 & 15 – gas sampling valve).

2.2. Multi–core reactor design

The reactor contained outer core for the pyrolysis of plastic, middle core as a heating zone and an inner core for synthesis of CNTs (Fig. 1). The heating coil placed in the middle core was covered with ceramic insulation wool of thickness 12.7 mm to increase heat flow in the inner core. In Fig. 2 half–sectional view of reactor shows inner chamber (high–temperature zone) to synthesize CNTs by CVD method. The tray arrangement in the CNT chamber provided maximum catalyst holdup. The up draft and cross flow of hydrocarbon gases across each plate of the holder increased the solid–gas contact.

The photographs of different cores and multi-core reactor assembly are presented for the reference (Fig. S1). The heating coil is directly wrapped over the CNT chamber so that it can achieve the temperature of 800 °C in 20 min. The thermal heat from the heating coil is transferred through the thin slayer of insulation to the inner wall of pyrolysis chamber (3 mm thick) by radiation. The heat transfer occurs from inner wall to the pyrolysis chamber by the mode of conduction. Pyrolysis chamber takes 120 min to attain the temperature of 700 °C due to larger volume as compared to the CNT chamber. The fins inside the pyrolysis chamber also increase the rate of heat transfer to the plastic mass.

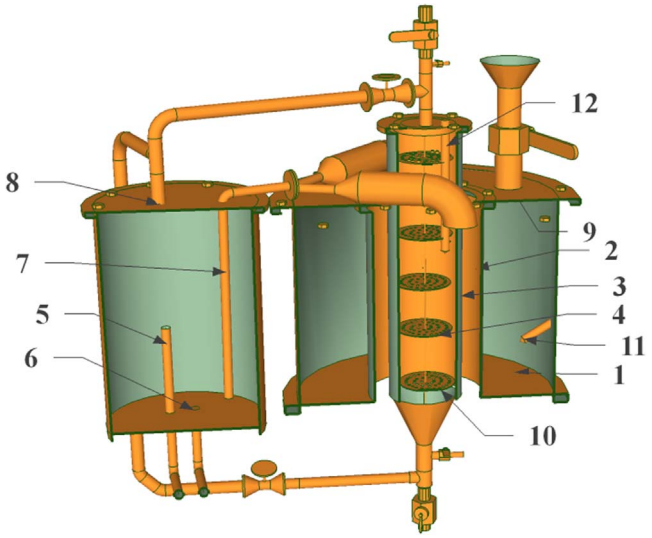

Fig. 2. Reactor cut section showing inner chambers and catalyst tray arrangement. (1 – pyrolysis chamber, 2 – heating chamber, 3 – CNT chamber, 4 – catalyst tray, 5 – oil drain line, 6 – water drain line, 7 – pyrolysis gas line to condenser, 8–non condensable gases to CNT chamber, 9 – Plastic feeder, 10 – first tray, 11 & 12 – thermo well).

The temperature of CNT chamber is maintained at 800 °C by using on/off controller. The experiments were performed after the desired temperature of pyrolysis chamber has been reached, with temperature fluctuation of ± 10 °C.

The condenser design provides direct purging of hydrocarbon gases into the water and circulation of non–condensable gases to the CNT chamber. Provision was made to send non–condensable gases to the CNT chamber from the top (downdraft flow) and from the bottom (up draft flow). In the present study, synthesis of CNTs was carried out using up draft flow of hydrocarbon gases.

2.3. Synthesis experiments

Ni/Mo/MgO catalyst of molar ratio 4/0.2/1 was prepared similar the procedure reported in our previous study[25].

Shredded plastic (5 × 5 cm) was fed into reactor when the reactor reached the desired temperature. The plastic was fed through the hopper provided at the top closure of pyrolysis chamber. The total plastic feed of 30 g was charged at a regular interval (5 g/2 min) into the pyrolysis chamber. Pyrolysis temperature was varied from 450 to 700 °C and optimum temperature of 800 °C for CNT chamber was used as per our earlier study [26]. Vapours from the pyrolysis chamber were condensed in the water purge tank and non–condensable vapours with a flow rate of 1–2 standard litter per minute (SLM) were sent to the CNT chamber. The condensed oil was collected from the oil drain valve provided at the bottom of condenser.

Each tray of holder was loaded with 0.2 g of catalyst and further kept in the CNT chamber at 800 °C. Air from both the chambers was evacuated using a vacuum pump. Non–condensable gases from the water purge tank were sent to the CNT chamber with the up–draft flow of 1–2 SLM, for 12 min. Tray filled with a black carbonaceous product was removed from the CNT chamber after 15 min. The tray was cooled to room temperature and the carbon product was removed and weighed.

2.4. Material characterization

The gas composition was analyzed by Gas Chromatography (Thermo Fisher Trace 1110 GC). The GC was equipped with thermal conductivity detector (TCD) and Flame ionization Detector (FID). TCD fitted with 10 feet length by 1/8 inch diameter column, MS.13X was used for the detection of H_2 and CO. The FID detector used for the analysis of hydrocarbon gases was fitted with 50 m × 0.32 mm × 5 µm (Agilent CP–Al_2O_3/KCl) column.

The liquid composition was analyzed by Gas Chromatography (Thermo Fisher Trace 1110 GC). The FID detector used for the analysis of hydrocarbon liquid was fitted with 50 m × 0.2 mm × 0.5 µm film thickness (SUPELCO, Petrocol™ DH 50.2, Fused silica) capillary column. The test conditions were kept similar to the PIONA quantitative analytical standard Supelco, n-paraffin mix (catalogue No. 48265-U) and peaks were identified using Hydrocarbon Expert V5.06.

The FTIR spectra for oil were recorded using a Shimadzu spectrophotometer(Japan) at a resolution of 4 cm^{-1} in the range of 500–4000 cm^{-1}. Microscopic structures of the CNTs were obtained using A– Tecnai G2F30 transmission electron microscopy at 300 kV. The Raman spectroscopy of CNTs was obtained using a Thermo–Nicolet 6700 HR 800 spectrometer in the range of 200–3000 cm^{-1}.

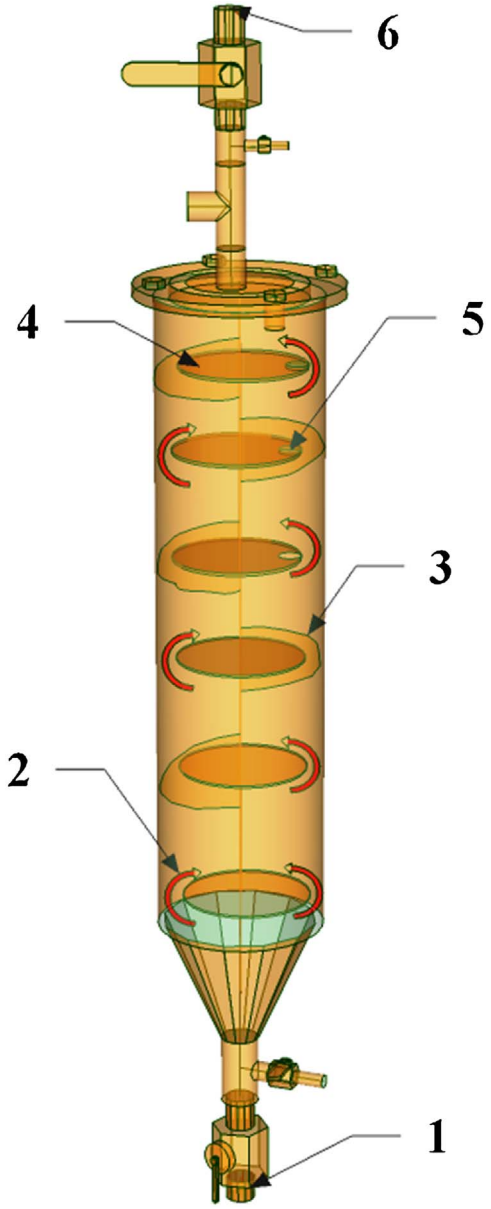

Fig. 3. The gas flow direction along the chamber wall and across the catalyst tray. (1 – gas inlet, 2 – gas flow direction, 3 – ceramic wool packing, 4 – tray no. 6, 5 – thermo well insertion whole, 6 – gas outlet).

3. Result and discussion

3.1. Batch production of CNTs

The study aims to make use of all hydrocarbons generated from pyrolysis of plastic waste to produce fuel oil and CNTs. Experiments were carried out to study the effect of pyrolysis temperature on the yield of gas, oil and CNTs.

The material of construction and fabrication details for different chambers is given in supplementary data (see Table S1). Pyrolysis chamber was designed to occupy polymeric material up to 3 kg. A hopper arrangement was provided for continuous feeding of plastic material to the pyrolysis chamber. The CNT section was designed as vertical chamber with catalyst tray arrangement. The tray was made up of SS 304 material having six circular plates of diameter 60 mm with a distance of 72 mm between two plates.

In the CNT chamber, the gap between chamber wall and edge of tray were sealed using ceramic wool (Fig. 3). The red arrow indicates

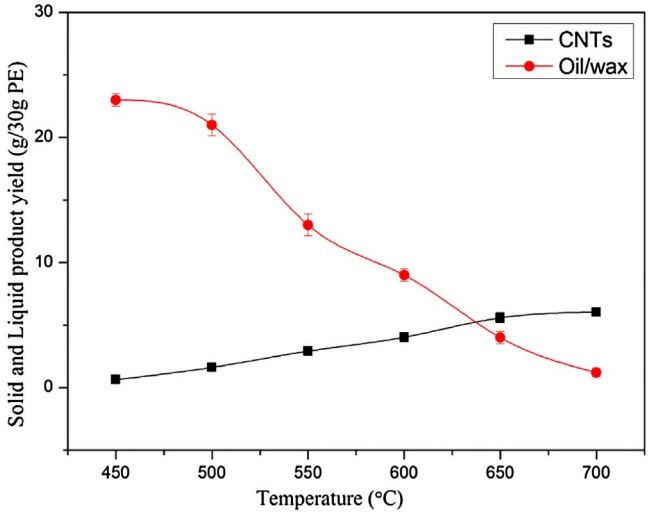

Fig. 4. Effect of pyrolysis temperature on the yield of oil and CNTs (CNT chamber maintained at constant temperature of 800 °C).

gas flow direction through the sidewall and across the plate. The sealing was staggered on each plate to prevent channeling of gas along the periphery of reactor wall and to increase gas solid interaction on each plate. When the hydrocarbon gas contacts the catalyst particles, it dissociates into carbon and hydrogen by catalytic decomposition. The dissociated carbon further diffuses into the catalyst and the growth of CNT occurs by precipitating carbon atoms.

The temperature profile for the pyrolysis chamber and CNT chamber is given in supplementary data (see Fig. S2). The heating coil (Kanthal Wire of 2000 W) was provided in the annulus to heat both the chambers and the heating was controlled using PID controller. An additional heater (Kanthal Wire of 1000 W) underneath pyrolysis chamber was used at the initial stage of operation to increase heating rate.

The effect of pyrolysis temperature on the yield of oil and CNTs is shown in Fig. 4. Increase in pyrolysis temperature from 450 to 700 °C, the oil yield decreased from 20 to 1.2 g/30 g PE, while the CNT yield increased from 0.23 to 6.033 g/30 g PE. Miskolczi et al. [27] reported that the degradation product of PE at the higher temperatures mainly yields methane, ethane, ethylene, propylene and hydrogen, which considerably increased the gas volume and lowers the oil yield [28]. The CNT yield was varied due to change in composition of pyrolysis gases at different pyrolysis temperatures [20].

The carbon weight retained on various trays at different pyrolysis temperature is shown in Fig. 5. The result indicates variation in the carbon products retained on different trays and the carbon yield increased with the increase in pyrolysis temperature. First tray located at the bottom showed maximum carbon product and the carbon yield decreased on subsequent trays. This is plausibly due to the updraft flow of non-condensable gases in the CNT chamber. The hydrocarbon vapours rich in carbon source may encounters with the catalyst on the first tray and the growth of CNTs occurs through the release of hydrogen gas. Further, the hydrogen–rich hydrocarbon gas travels further to the subsequent trays and interact with catalyst. The decrease in carbon source in the gaseous stream could be the reason for the decrease in CNT yield in subsequent trays. The result showed maximum carbon product of 2.13 g for the first tray and total carbon yield of 6.033 g/30 g PE over entire catalyst tray at pyrolysis temperature of 700 °C.

The composition of gases obtained from pyrolysis of PE at different pyrolysis temperature was determined by gas chromatography (Fig. 6a). The concentration of hydrogen and methane increased from 2.18 to 23.64 Vol.% and 12.60 to 27.66 Vol.% respectively with increase in pyrolysis temperature from 450 °C to 700 °C. However,

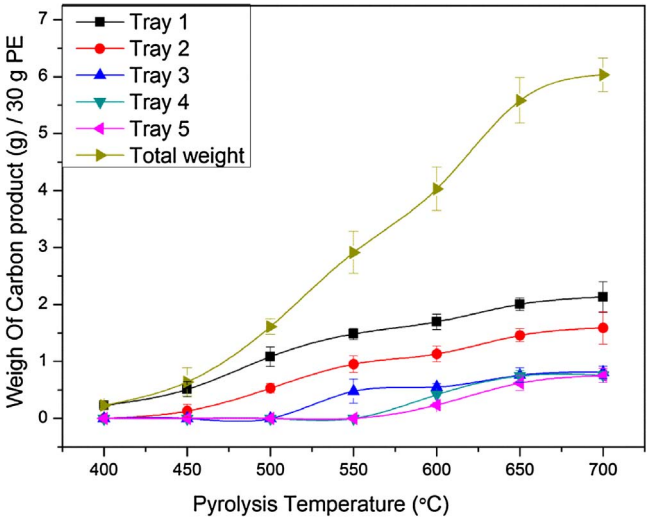

Fig. 5. Weight of carbon product collected from various trays at different pyrolysis temperature.

the concentrations of C_2–C_5 decreased with the increase in pyrolysis temperature. The result indicates that, PE decomposes to unsaturated hydrocarbons at lower pyrolysis temperature and gives more oil yield. Whereas at high temperature, cracking of unsaturated gases (alkenes) occurred and generated more methane and hydrogen. The less amount of carbon product at lower pyrolysis temperature (Fig. 5) indicated that unsaturated gases were unfavorable for the growth of CNTs.

The gases obtained at different pyrolysis temperature were utilized to synthesize CNTs at a fixed temperature of 800 °C. In Fig. 6b composition of gases obtained from CNT chamber is plotted as a function of pyrolysis temperature. The result showed small variations in the Vol.% of all gases at different temperature range. The gas contained major proportion of hydrogen and methane, while ethane, ethylene and CO were observed to be in trace amount.

The traces of CO (0.59–2.07 Vol.%) can be observed at different temperature range due to air inclusion while feeding the plastic in the reactor. The gas chromatogram in Fig. 7 shows presence of CO in the gases sample obtained at pyrolysis temperature of 450, 600, 700 °C.

The effect of thermal and catalytic decomposition can be understood by comparing Fig. 6a and b. In the pyrolysis chamber, due to thermal decomposition at 700 °C the product gases contained 23.64 Vol.% Hydrogen, 27.66 Vol.% Methane and other hydrocarbon

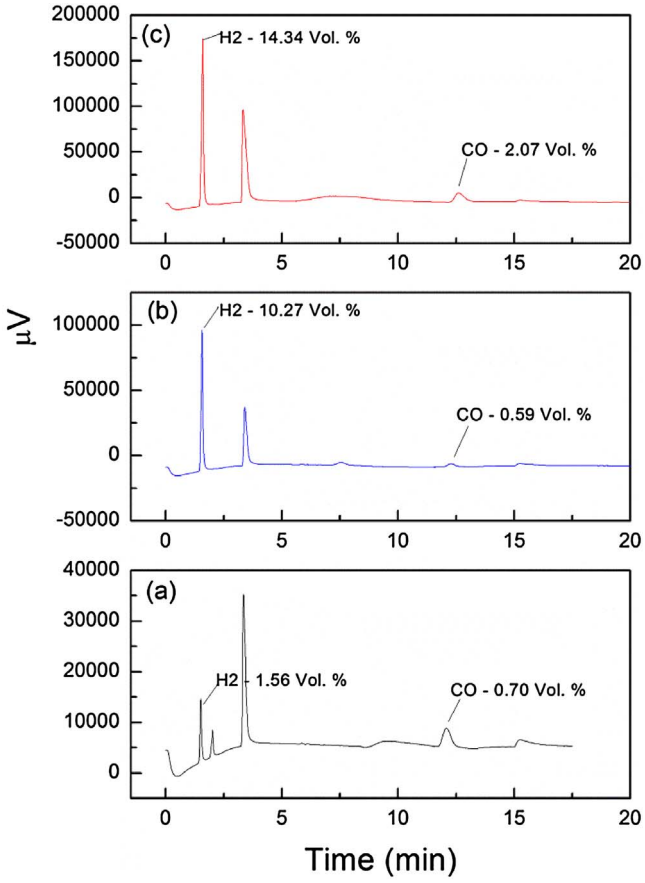

Fig. 7. Gas chromatogram showing presence of H_2 and CO in the gases sample obtained at pyrolysis temperature of (a) 450, (b) 600, (c) 700 °C.

gases. While sending these gases to CNT chamber, the hydrogen gas increased to 75.37 Vol.%. It is worth noting that both thermal and catalytic decomposition of gases occurs in CNT chamber. Mainly the unsaturated hydrocarbon gases from lower pyrolysis temperature were thermally decomposed to methane and hydrogen and further the methane was cracked to individual carbon atom and hydrogen by catalytic decomposition at 800 °C.

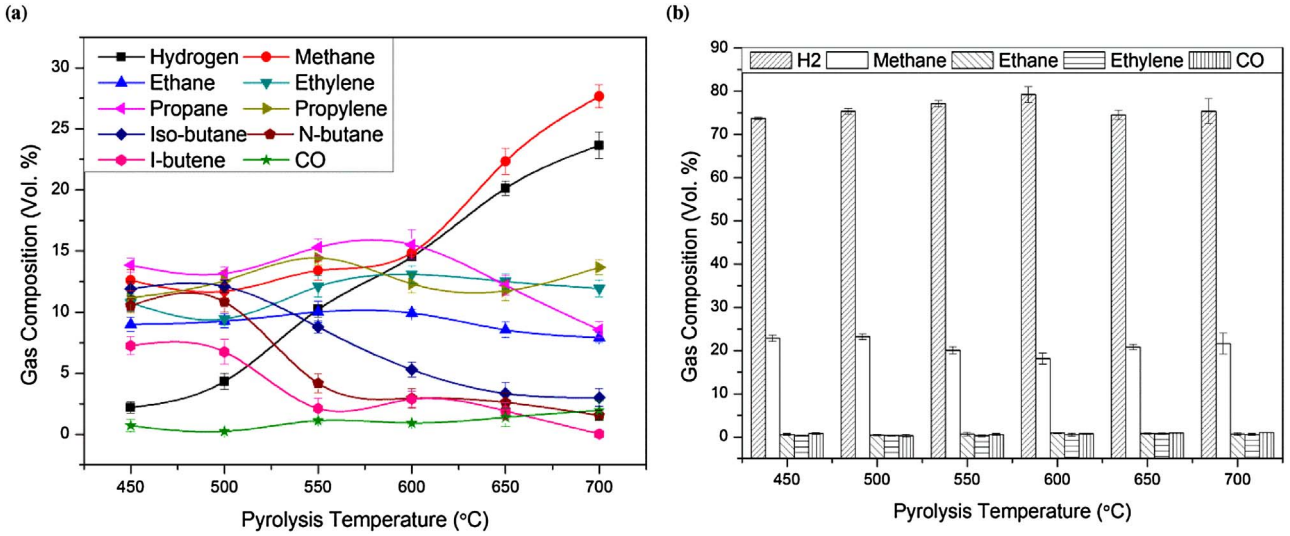

Fig. 6. (a) Composition of gases product obtained from pyrolysis chamber as a function of temperature, (b) Composition of gases product obtained from CNT chamber (800 °C) at different pyrolysis temperature.

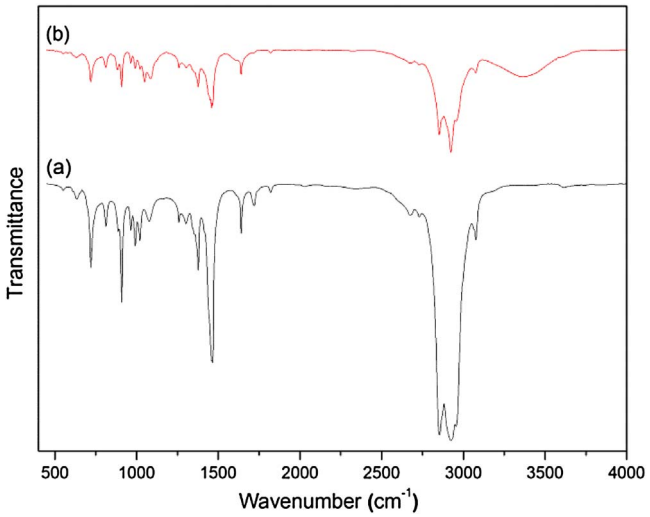

Fig. 8. FTIR spectroscopy of oil obtained from pyrolysis of waste HDPE cans at 450 °C (a) and 550 °C (b).

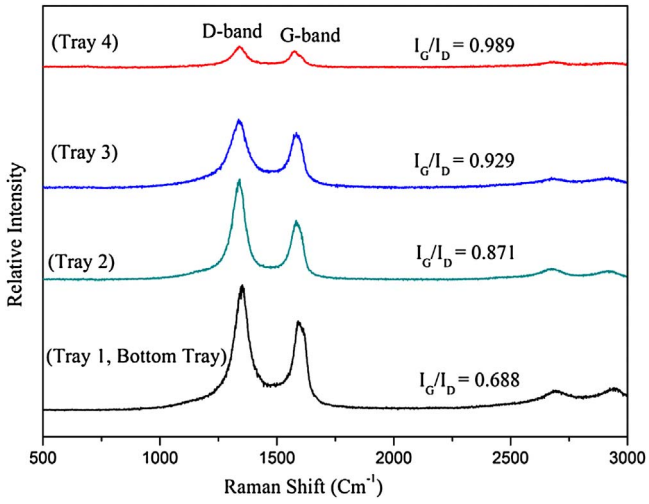

Fig. 10. Raman spectra of CNTs synthesize over $Ni_4Mo_{0.2}MgO_1$ catalyst on different trays.

3.2. Characterization of condensed oil

3.2.1. FTIR analysis of oil

The FTIR spectra for the oil obtained from pyrolysis of waste HDPE cans at 450 °C and 550 °C are shown in Fig. 8(a and b) respectively. The symmetric and asymmetric stretching bands of C—H bonds corresponding to alcoholic $-CH_2$ bond around 2853, 2924 and 1458 cm^{-1} are similar to the bond present in commercial waxes [29,30].

The band around 3076 cm^{-1} occurs due to presence of aromatic —C—H bond. The bands around 1377 cm^{-1} corresponding to the aliphatic chains are due to the vibration of CH_2 or $-CH_3$ bend. The peak at 991 cm^{-1} show the presence of vinyl —C—H bond in mono substituted alkenes. The olefinic nature of pyrolysis oil/waxes was confirmed by the presence of R—CH=CH_2 group at 908, 991 cm^{-1}. The peak at 1640 cm^{-1} can be attributed to the C=C stretching vibrations in the polyaromatic compounds. The band around 1600–1450 cm^{-1}, 850–660 cm^{-1} and the characteristic pattern in the overtone region around 2000–1800 cm^{-1} are related to mono − substituted aromatic compound [29,30]. The peaks at 552, 632, 812 cm^{-1} respectively shows the presence of alkyl halides, vinyl —C—H and vinyl ethers in the pyrolysis sample. The spectrum is similar to that of the oil prepared from pure polyethylene by Arabiourrutia et al. [31].

3.2.2. GC analysis of oils

In this study, oil compositions obtained from pyrolysis of HDPE have been evaluated by gas chromatography. The detailed component analysis is shown in Tables S2 and S3. The distribution of compounds was determined using percentage area of chromatographic peaks. Fig. 9a–c shows the GC profile for the composition of liquid product obtained from pyrolysis of HDPE at 500, 600, 700 °C respectively. The liquid product obtained at different pyrolysis temperature contained alkanes, long chain olefins and aromatics which occur due to thermal degradation of PE by the formation of free radicals and cracking of C—C and C—H bonds [32]. The result showed higher yield of aromatic and cyclic compounds (83–85%) than aliphatic compounds (14–16%). This

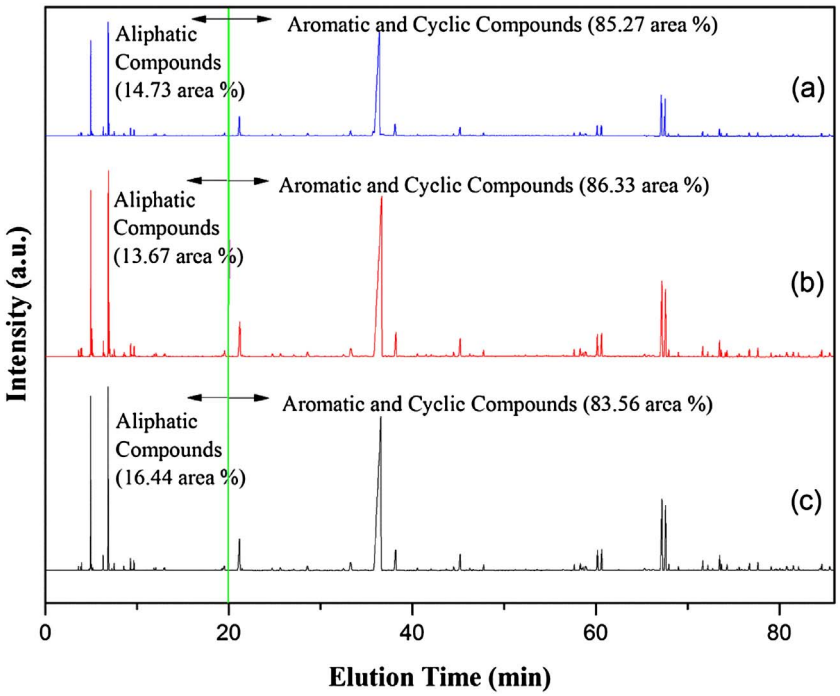

Fig. 9. Gas chromatogram showing composition of liquid product obtained at pyrolysis temperature of (a) 500, (b) 600, (c) 700 °C.

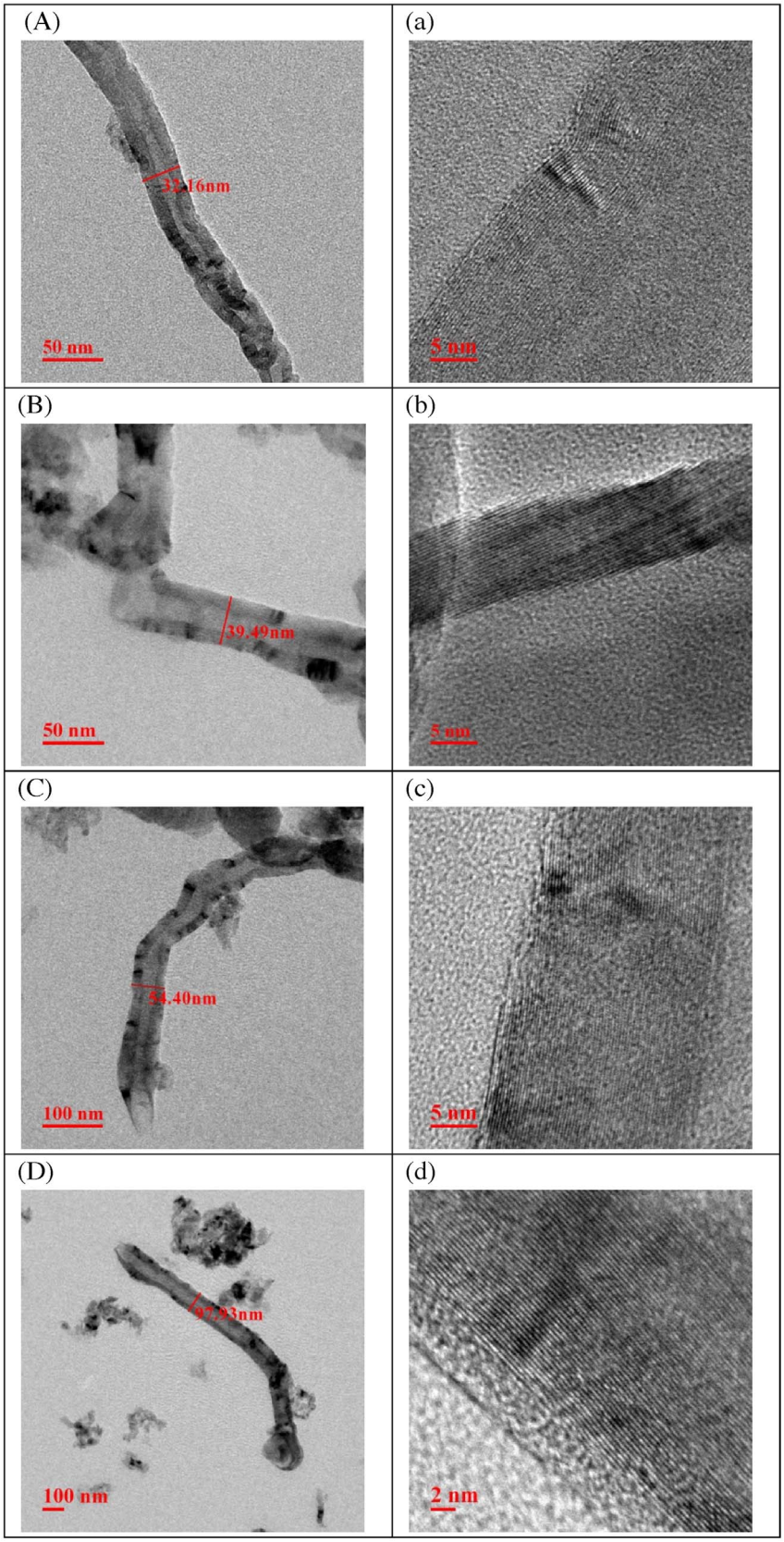

Fig. 11. HRTEM image of CNTs synthesized over $Ni_4Mo_{0.2}MgO_1$ catalyst on different trays (A, B, C, D tray number 4, 3, 2, 1 respectively), Pyrolysis chamber at 650 °C and CNT chamber at 800 °C.

could be due to the formation of aromatics by the secondary reactions such as oligomerization, cyclization and dehydrogenation of olefins [32].

3.3. Characterization of catalyst and CNTs

The characterization of catalyst $Ni_4Mo_{0.2}MgO_1$ was studied in detail elsewhere [26]. The Raman spectrum of CNTs in Fig. 10 shows small variations in the peak intensity ratio of G–band and D–band (I_G/I_D) on different trays. The larger I_G/I_D ratio indicates a higher degree of structural ordering for CNTs [33,34]. The ratio was found to be increasing from bottom to top tray. This could be because the catalyst $Ni_4Mo_{0.2}MgO_1$ kept on the various trays exposed to the gases containing different proportions of hydrocarbons. The decomposition of saturated hydrocarbons to carbon and hydrogen and unsaturated hydrocarbons to saturated hydrocarbons could occur on the first tray. The catalyst on the second tray could expose to the hydrocarbon containing more amount of hydrogen and saturated hydrocarbon like methane and ethane. Similar observations for the variation in the trend of CNT yield using two stage reactor at different composition of gases was reported by Liu et al. [20].

The HRTEM images of CNTs collected from different tray (A − 4th tray and D − 1st tray, bottom tray) are shown in Fig. 11A–D. The morphological study of CNTs collected from various trays indicated random growth of tubes over Ni/Mo/MgO catalyst. The growth of CNTs could occur by base–growth mechanism having a hollow structure, which appears as a continuous white line in Fig. 11. The catalyst on the top tray exposed to the hydrocarbon containing more amount of hydrogen which lead to the better aligned graphene walls than the bottom tray [35].

The HRTEM study shows small variation in the diameter of CNTs. The bottom tray contained CNTs having 50–55 nm inner diameter and 95–100 nm outer diameter. Subsequently tray number 2, 3, 4 contained CNTs having inner/outer diameter of 20–25/50–60 nm, 15–20/35–45 nm and 10–15/25–35 nm respectively. The 4th tray of CNT chamber exposed to the more amount of hydrogen gas, which was liberated from the CNT synthesis process from preceding trays. This hydrogen could reduced the NiO present in the catalyst to Ni metal ion and subsequently interacted with unreacted hydrocarbon gases, thereby altered the rate of carbon supply to the catalyst particles [36].

4. Conclusion

A facile multi–core reactor design has been proposed for the efficient production of CNTs. Batch synthesis of CNTs was successfully carried out using waste plastic as a hydrocarbon source and Ni/Mo/MgO as a catalyst. Pyrolysis temperatures affected the yield of fuel oil and CNTs. The maximum yield of CNTs was 6.033 g/30 g PE at a feed rate of 5 g/2 min at a pyrolysis temperature of 700 °C and CNT synthesis temperature of 800 °C. The maximum yield of oil was 23 g/30 g PE at 450 °C but at this temperature, the CNT yield was very low. The CNTs collected from different trays showed variations in the diameter. However, the present study helps to understand the changes in morphology of CNTs at different height of the reactor.

Acknowledgement

Vijayakumar R.P. is thankful to Science and Engineering Research Board, Government of India for providing SERB − Young Scientist Fellowship (Project no. SB/FTP/ETA–0235/2013).

Appendix A. Supplementary data

Supplementary data associated with this article can be found, in the online version, at http://dx.doi.org/10.1016/j.jaap.2017.04.016.

References

[1] E.F.F. Kukovitskii, L.A.A. Chernozatonskii, S.G.G. L'vov, N.N.N. Mel'nik, Carbon nanotubes of polyethylene, Chem. Phys. Lett. 266 (1997) 323–328, http://dx.doi.org/10.1016/S0009-2614(97)00020-1.
[2] G.R. Li, F. Wang, Q.W. Jiang, X.P. Gao, P.W. Shen, Carbon nanotubes with titanium nitride as a low-cost counterelectrode material for dye-sensitized solar cells, Angew. Chem. Int. Ed. 49 (2010) 3653–3656, http://dx.doi.org/10.1002/anie.201000659.
[3] L. c Yang, B.H. Fishbine, A. Migliori, L.R. Pratt, Molecular simulation of electric double-layer capacitors based on carbon nanotube forests, J. Am. Chem. Soc. 131 (2009) 12373–12376, http://dx.doi.org/10.1021/ja9044554.
[4] D. Eder, Carbon nanotube-inorganic hybrids, Chem. Rev. 110 (2010) 1348–1385, http://dx.doi.org/10.1021/cr800433k.
[5] Y. Huang, J. Liang, Y. Chen, An overview of the applications of graphene-based materials in supercapacitors, Small 8 (2012) 1805–1834, http://dx.doi.org/10.1002/smll.201102635.
[6] M. Paradise, T. Goswami, Carbon nanotubes − production and industrial applications, Mater. Des. 28 (2007) 1477–1489, http://dx.doi.org/10.1016/j.matdes.2006.03.008.
[7] A. Javey, J. Guo, Q. Wang, M. Lundstrom, H. Dai, Ballistic carbon nanotube field-effect transistors, Nature 424 (2003) 654–657, http://dx.doi.org/10.1038/nature01797.
[8] A. Bazargan, G. McKay, A review − synthesis of carbon nanotubes from plastic wastes, Chem. Eng. J. 195-196 (2012) 377–391, http://dx.doi.org/10.1016/j.cej.2012.03.077.
[9] Z. Shi, Y. Lian, X. Zhou, Z. Gu, Y. Zhang, S. Iijima, et al., Mass-production of single-wall carbon nanotubes by arc discharge method, Carbon N. Y. 37 (1999) 1449–1453, http://dx.doi.org/10.1016/S0008-6223(99)00007-X.
[10] W.K. Maser, E. Muñoz, A.M. Benito, M.T. Martínez, G.F. de la Fuente, Y. Maniette, et al., Production of high-density single-walled nanotube material by a simple laser-ablation method, Chem. Phys. Lett. 292 (1998) 587–593, http://dx.doi.org/10.1016/S0009-2614(98)00776-3.
[11] K. Dasgupta, R. Venugopalan, G.K. Dey, D. Sathiyamoorthy, Novel catalytic route to bulk production of high purity carbon nanotube, J. Nanopart. Res. 10 (2008) 69–76, http://dx.doi.org/10.1007/s11051-007-9219-5.
[12] R. Andrews, D. Jacques, A.M. Rao, F. Derbyshire, Continuous production of aligned carbon nanotubes: a step closer to commercial realization, Chem. Phys. Lett. 303 (1999) 467–474, http://dx.doi.org/10.1016/S0009-2614(99)00282-1.
[13] P. Nikolaev, M.J. Bronikowski, R.K. Bradley, F. Rohmund, D.T. Colbert, K. a Smith, et al., Gas-phase catalytic growth of single-walled carbon nanotubes from carbon monoxide, Chem. Phys. Lett. 313 (1999) 91–97, http://dx.doi.org/10.1016/S0009-2614(99)01029-5.
[14] H.J. Jeong, K.K. Kim, S.Y. Jeong, M.H. Park, C.W. Yang, Y.H. Lee, High-yield catalytic synthesis of thin multiwalled carbon nanotubes, J. Phys. Chem. B 108 (2004) 17695–17698, http://dx.doi.org/10.1021/jp046152o.
[15] Y. Li, X.B. Zhang, X.Y. Tao, J.M. Xu, W.Z. Huang, J.H. Luo, et al., Mass production of high-quality multi-walled carbon nanotube bundles on a Ni/Mo/MgO catalyst, Carbon N. Y. 43 (2005) 295–301, http://dx.doi.org/10.1016/j.carbon.2004.09.014.
[16] J. Gong, J. Liu, D. Wan, X. Chen, X. Wen, E. Mijowska, et al., Catalytic carbonization of polypropylene by the combined catalysis of activated carbon with Ni2O3 into carbon nanotubes and its mechanism, Appl. Catal. A Gen. 449 (2012) 112–120, http://dx.doi.org/10.1016/j.apcata.2012.09.028.
[17] Q. Zhang, J.Q. Huang, M.Q. Zhao, W.Z. Qian, F. Wei, Carbon nanotube mass production: principles and processes, ChemSusChem 4 (2011) 864–889, http://dx.doi.org/10.1002/cssc.201100177.
[18] C. Zhuo, B. Hall, Y. Levendis, H. Richter, A novel technology for green(er) manufacturing of CNTs via recycling of waste plastics, MRS Proc. 1317 (2011) 1–6, http://dx.doi.org/10.1557/opl.2011.139.
[19] C. Zhuo, B. Hall, H. Richter, Y. Levendis, Synthesis of carbon nanotubes by sequential pyrolysis and combustion of polyethylene, Carbon N. Y. 48 (2010) 4024–4034, http://dx.doi.org/10.1016/j.carbon.2010.07.007.
[20] J. Liu, Z. Jiang, H. Yu, T. Tang, Catalytic pyrolysis of polypropylene to synthesize carbon nanotubes and hydrogen through a two-stage process, Polym. Degrad. Stab. 96 (2011) 1711–1719, http://dx.doi.org/10.1016/j.polymdegradstab.2011.08.008.
[21] U. Arena, M.L. Mastellone, G. Camino, E. Boccaleri, An innovative process for mass production of multi-wall carbon nanotubes by means of low-cost pyrolysis of polyolefins, Polym. Degrad. Stab. 91 (2006) 763–768, http://dx.doi.org/10.1016/j.polymdegradstab.2005.05.029.
[22] F. Danafar, A. Fakhru'l-Razi, M.A.M. Salleh, D.R.A. Biak, Fluidized bed catalytic chemical vapor deposition synthesis of carbon nanotubes – a review, Chem. Eng. J. 155 (2009) 37–48, http://dx.doi.org/10.1016/j.cej.2009.07.052.
[23] Q. Zhang, M.-Q. Zhao, J.-Q. Huang, Y. Liu, Y. Wang, W.-Z. Qian, et al., Vertically aligned carbon nanotube arrays grown on a lamellar catalyst by fluidized bed catalytic chemical vapor deposition, Carbon N. Y. 47 (2009) 2600–2610, http://dx.doi.org/10.1016/j.carbon.2009.05.012.
[24] D.Y. Kim, H. Sugime, K. Hasegawa, T. Osawa, S. Noda, Sub-millimeter-long carbon nanotubes repeatedly grown on and separated from ceramic beads in a single fluidized bed reactor, Carbon N. Y. 49 (2011) 1972–1979, http://dx.doi.org/10.1016/j.carbon.2011.01.022.
[25] D.A. Ward, E.I. Ko, Preparing catalytic materials by the sol-gel method, Ind. Eng. Chem. Res. 34 (1995) 421–433, http://dx.doi.org/10.1021/ie00041a001.
[26] G.S. Bajad, S.K. Tiwari, R.P. Vijayakumar, Synthesis and characterization of CNTs using polypropylene waste as precursor, Mater. Sci. Eng. B 194 (2015) 68–77, http://dx.doi.org/10.1016/j.mseb.2015.01.004.

[27] N. Miskolczi, F. Ateş, N. Borsodi, Comparison of real waste (MSW and MPW) pyrolysis in batch reactor over different catalysts. Part II: contaminants, char and pyrolysis oil properties, Bioresour. Technol. 144 (2013) 370–379, http://dx.doi.org/10.1016/j.biortech.2013.06.109.
[28] M.A. Nahil, C. Wu, P.T. Williams, Influence of metal addition to Ni-based catalysts for the co-production of carbon nanotubes and hydrogen from the thermal processing of waste polypropylene, Fuel Process. Technol. 130 (2015) 46–53, http://dx.doi.org/10.1016/j.fuproc.2014.09.022.
[29] A. Chaala, H. Darmstadt, C. Roy, Vacuum pyrolysis of electric cable wastes, J. Anal. Appl. Pyrolysis 39 (1997) 79–96, http://dx.doi.org/10.1016/S0165-2370(96)00964-3.
[30] A.R.T.S. Brains Furniss, Antony J. Hannaford, Peter W.G. Smith, Vogel's Textbook of Practicle Organic Chemistry, 5th ed., Longman Scientific & Technical, New York, 1989.
[31] M. Arabiourrutia, G. Elordi, G. Lopez, E. Borsella, J. Bilbao, M. Olazar, Characterization of the waxes obtained by the pyrolysis of polyolefin plastics in a conical spouted bed reactor, J. Anal. Appl. Pyrolysis 94 (2012) 230–237, http://dx.doi.org/10.1016/j.jaap.2011.12.012.
[32] J. Gong, J. Liu, Z. Jiang, J. Feng, X. Chen, L. Wang, et al., Striking influence of chain structure of polyethylene on the formation of cup-stacked carbon nanotubes/carbon nanofibers under the combined catalysis of CuBr and NiO, Appl. Catal. B Environ. 147 (2014) 592–601, http://dx.doi.org/10.1016/j.apcatb.2013.09.044.
[33] W.S. Bacsa, D. Ugarte, A. Châtelain, W.A. de Heer, High-resolution electron microscopy and inleastic light scattering of purified multishelled carbon nanotubes, Phys. Rev. B 50 (1994) 473–477, http://dx.doi.org/10.1103/PhysRevB.50.15473.
[34] N. Mishra, G. Das, A. Ansaldo, A. Genovese, M. Malerba, M. Povia, et al., Pyrolysis of waste polypropylene for the synthesis of carbon nanotubes, J. Anal. Appl. Pyrolysis 94 (2012) 91–98, http://dx.doi.org/10.1016/j.jaap.2011.11.012.
[35] I.V. Lebedeva, A.A. Knizhnik, A.V. Gavrikov, A.E. Baranov, B.V. Potapkin, S.J. Aceto, et al., First-principles based kinetic modeling of effect of hydrogen on growth of carbon nanotubes, Carbon N. Y. 49 (2011) 2508–2521, http://dx.doi.org/10.1016/j.carbon.2011.02.021.
[36] R. Brukh, S. Mitra, Mechanism of carbon nanotube growth by CVD, Chem. Phys. Lett. 424 (2006) 126–132, http://dx.doi.org/10.1016/j.cplett.2006.04.028.